CDK1/FBXW7 Facilitates Degradation and Ubiquitination of MLST8 to Inhibit Progression of Renal Cell Carcinoma

Encheng Zhang
Shanghai Jiaotong University: Shanghai Jiao Tong University
Xiao Dong
Shanghai Jiaotong University: Shanghai Jiao Tong University
Jialiang Shao
Shanghai Jiaotong University: Shanghai Jiao Tong University
Xingyu Mu
Shanghai jiaotong university
Siteng Chen
Shanghai Jiaotong University First People's Hospital
Yuqi Wang
Fudan University School of Life Sciences
Pingzhao Zhang
Fudan University School of Life Sciences
mingyue Tan
Shanghai Jiaotong University: Shanghai Jiao Tong University
Qing Shi
Fudan University School of Life Sciences
Xiang Wang (drseanwang@163.com)
Shanghai Jiaotong University First People's Hospital

Research

Keywords: FBXW7, MLST8, CDK1, renal cell carcinoma, protein degradation, ubiquitination

Posted Date: October 30th, 2020

DOI: https://doi.org/10.21203/rs.3.rs-97872/v1

Version of Record: A version of this preprint was published at Cancer Science on November 5th, 2021. See the published version at https://doi.org/10.1111/cas.15188.

Abstract

Background: Recent studies have reported that MLST8 is upregulated in many malignant tumors. Nevertheless, the underlying molecular mechanisms is still unclear. The aim of this work was to investigate how MLST8 contribute to the development and progression of renal cancer (ccRCC).

Methods: To identify molecular mediators of the oncogenic tumor function of MLST8, we analyzed a quantitative mass spectrometry by a previous study and checked the amino acid sequence in MLST8. Immunoprecipitation and Western Blotting were used to analyze the interaction between FBXW7 and MLST8. Transwell assays determined cell migration and invasion. *In vivo* experiments were performed to verify tumor growth. Immunohistochemistry was used to analyze protein levels in patients' tumor samples.

Results: MLST8 is an oncogenic protein in TCGA database and ccRCC clinical specimens. We also ascertain that MLST8 interacts with FBXW7, which was universally regarded as an E3 ubiquitin ligase. MLST8 can be degraded and ubiquitinated by tumor suppressor FBXW7. FBXW7 recognizes a consensus motif (T/S) P*XX* (S/T/D/E) of MLST8 and triggers MLST8 degradation via the ubiquitin-proteasome pathway. Strikingly, the activated CDK1 kinase engages in the MLST8 phosphorylation required for FBXW7-mediated degradation. *In vitro and vivo* assay, we further prove that MLST8 is an essential mediator of FBXW7 inactivation-induced tumor growth, migration, and invasion. Furthermore, MLST8 and FBXW7 protein are negatively correlated in human renal cancer specimens.

Conclusions: Our findings suggest that MLST8 is a putative oncogene that functions via interaction with FBXW7, and inhibition MLST8 can be a potential future target in ccRCC treatment.

Background

MTOR associated protein (MLST8), also known as G protein beta subunit-like (GBL), is a core component of mTORC1 and mTORC2, and contributes to the occurrence and progression of many tumors, including hepatocellular carcinoma (HCC) and colon cancer [1-3]. A previous study has shown that the depletion of MLST8 significantly suppresses mTORC1 and mTORC2 complex formation, resulting in slowing tumor growth and progression into human colon carcinomas and prostate cancer cells [4]. MLST8 has been reported to promote the proliferation and invasion of hepatocellular carcinoma cells through the AKT pathway [5]. Mouse embryo knockout experiments demonstrate an essential role of MLST8 in mTORC2 and directly affects mTORC2's function [6].

F-box and WD repeat domain-containing 7 (FBXW7) is the substrate recognition component of the Skp1-Cul1-F-box (SCF) ubiquitin ligase complex. It recognizes and binds to its substrates via the conserved Cdc4-phosphodegron (CPD) motif (T/S-P-X-X-S/T/ D/E) [7]. In most instances, recognition of CPDs by FBXW7 is regulated by phosphorylation of individual amino acid residues residing within CPD motifs of the substrates [7]. FBXW7 targets multiple oncoproteins for ubiquitination and degradation, including cyclin E [8], c-Myc [9], c-Jun [10], Notch-1 [11], and SREBP1[12]. Studies have reported that the

suppression of FBXW7 stimulates the proliferation of tumor cells, attenuates apoptosis, abducts chromosome instability, and maintains stem-cell properties, all of which facilitates tumorigenesis [13, 14] . The mutant frequency of FBXW7 is 35% in twenty CCA patients [13]. Silencing of FBXW7 expression was found to render metabolic advantages in pancreatic cancer cells through the induction of aerobic glycolysis by downregulating the thioredoxin interacting protein (TXNIP) in a c-Myc dependent manner [15]. A previous study has demonstrated that decreased FBXW7 expression induces cancer antigen 125 (CA125) or Muc16 production in pancreatic cancer cells, which are both regarded as metastatic markers of pancreatic cancer cells [16].

A previous study used quantitative mass spectrometry of FBXW7 knockout (KO) HCT116 cells to authenticate MLST8 as a candidate substrate to FBXW7 [17]. In this study, we present data highlighting a crucial role of MLST8 towards tumor progression. We validate that FBXW7 physically interacts with MLST8 and mediates its ubiquitylation. Furthermore, we find that activated CDK1 kinase is involved in MLST8 phosphorylation, which is required for FBXW7-mediated MLST8 degradation. We show that MLST8 and FBXW7 protein levels are negatively correlated in ccRCC patient specimens. Taken together, our results are conducive to a more complete understanding of the regulatory mechanism of MLST8 in human ccRCC. These understanding highlights potential future efforts towards developing therapeutic strategies against ccRCC.

Materials And Methods

Cell culture and transfection

786-O, A498, and 293T cells were obtained from the American Type Culture Collection (ATCC). 786-O cells were cultured in RPMI 1640 medium supplemented with 10% fetal bovine serum (FBS) 100 U/ml penicillin, and 100 μg/ml streptomycin, and incubated in a 5% CO2 humidified incubator at 37°C. A498 and 293T cells were cultured in DMEM medium supplemented with 10% FBS. All transient transfections were performed using Lipofectamine 2000 (Invitrogen) according to the manufacturer's instructions. Determine the contribution of cyclin B-CDK1, and cells were treated with a CDK inhibitor, such as butyrolactone I [18, 19] or RO-3306 (Calbiochem).

Expression constructs

Human cDNAs for c-Myc, Fbxw7, and MLST8 were amplified from the human brain cDNA library (Clontech) by polymerase chain reaction (PCR). These cDNAs were inserted into the *EcoR*I and *Not*I restriction sites of pCMV-HA vector, pCMV-FLAG vector, and pCMV-Myc. PCR amplified cDNAs for the phosphorylation site mutants of the mouse (T50A/S54A) and human (T50A) with primers corresponding to the mutant sequences and inserted into *Eco*RI/*BamH*I sites of pCMV-HA vector to generate pCMV-HA-c-Myc (T50A/S54A) and pCMV-HA-c-Myc (T50A), respectively. All the constructs were confirmed by DNA sequencing.

Establish stably Cas-9 knockout and overexpression 786-O cell line

The FBXW7 and MLST8 Cas-9 gene knockout plasmid was constructed using the Lenti CRISPR V2 plasmid, then transfected with psPAX2 and pCMV-VSV-G plasmid at a ratio of 4:3:3 into 293 T cells. 786-O cells in a 60mm dish were infected with 1 mL of virus supernatant when the cell density is 60–80%. The positive cells were screened with puromycin for two weeks. The result was verified by western blot. The method is the same as the above. 10μg pCDH-CD513B-Flag-FBXW7 plasmid, 10μg pCDH-CD513B-Myc-MLST8 plasmid respectively, and 10 μL of Lipofectamine 2000 were transfected into 786-O cells, then screened with puromycin for two weeks. The primer sequences were listed in Supplementary Table S1.

Antibodies

Commercially available antibodies for Western Blotting were as follows: FBXW7 (A5872, ABclonal), MLST8 (A13599, ABclonal), Myc (9E10; Sigma), FLAG (M2; Sigma), HA (MM5-101R; Millipore), and Actin (M20011; Abmart). Anti-human MLST8 phosphorylated Thr50 polyclonal antibody (anti-p-T50-MLST8) was raised against keyhole limpet hemocyanin-conjugated chemically synthesized phosphorylated Thr50 peptide, corresponding to the CPD region of MLST8 (aa residues 50–61) (MBL). Antiserum obtained from an immunized guinea pig was bound to column chromatography conjugated with P-T50 peptide. The affinity-purified anti-p-T50-MLST8 was then passed through a column conjugated to non-phosphorylated Thr50 peptide (aa residues 50–61 of MLST8) to deplete antibodies against the non-phosphorylated antigen. ELISA confirmed the specific binding ability of the purified antibody to P-T50 peptide.

Immunoprecipitation

To immunoprecipitate the ectopically expressed Flag-tagged proteins, transfected cells were lysed 24 h post-transfection in BC100 buffer. The whole-cell lysates were immunoprecipitated with the monoclonal anti-Flag antibody-conjugated M2 agarose beads (Sigma) at 4°C overnight. After three washes with Flag lysis buffer, followed by two washes with BC100 buffer, the bound proteins were eluted using Flag-Peptide (Sigma)/BC100 for 3 h at 4°C. SDS-PAGE resolved the eluted material. To immunoprecipitate the endogenous proteins, cells were lysed with 1× cell lysis buffer (Cell Signaling), and the lysate was centrifuged. The supernatant was precleared with protein A/G beads (Sigma) and incubated with indicated antibodies overnight. After that, protein A/G beads were applied, all at 4°C. After 2 h of incubation, pellets were washed five times with lysis buffer and resuspended in sample buffer and analyzed by SDS-PAGE.

In Vitro phosphorylation assay

GST-fused WT or T50A mutant of MLST8 was produced in *Escherichia coli* BL21 and purified using glutathione-Sepharose beads (GE Healthcare). *In vitro,* phosphorylation was described previously [20-22]. Eachrecombinant MLST8 was incubated with the indicated kinasesources, including recombinant cyclin D3-CDK4 (ab271459, Abcam), cyclin E1-CDK5 (ab56282, Abcam), cyclin A2-CDK2 (ab196060, Abcam), cyclin B1-CDK1 (ab271456, Abcam), or synchronized 786-O cell lysates at30 °C for 30 min in reaction buffer containing 1 mM ATP. The reaction was terminated by boiling with SDS-sample buffer for 8 min.

For *in vitro* phosphorylation following binding assays, phosphorylated mixtures were incubated for an additional 1 h at 4 °C with lysates from HEK293 cells exogenously expressing Fbxw7. GST-fused proteins were then precipitated using glutathione-Sepharose beads. The mixtures were treated with precision protease (GE Healthcare) for 30 min to cleave MLST8 from the GST tag. IB analyzed all reaction mixtures with the indicated antibodies.

Western blot

Cell lysates or immunoprecipitates were subjected to SDS-PAGE, and proteins were transferred to nitrocellulose membranes (GE Healthcare). The membranes were blocked in Tris-buffered saline (TBS, pH 7.4) containing 5% non-fat milk and 0.1% Tween-20, washed twice in TBS containing 0.1% Tween-20, and incubated with primary antibody for 2 h and followed by the secondary antibody for 1 h at room temperature. The proteins of interest were visualized using the ECL chemiluminescence system (Santa Cruz).

Quantitative RT-PCR

Total RNA was isolated from transiently transfected cells using the TRIzol reagent (Tiangen), and cDNA was reversed-transcribed using the Superscript RT kit (TOYOBO), according to the manufacturer's instructions. PCR amplification was performed using the SYBR Green PCR master mix kit (TOYOBO). All quantization was normalized to the level of endogenous control GAPDH. The primer sequences were listed in Supplementary Table S1.

CCK-8 assay

Cell proliferation rate was determined using Cell Counting Kit-8 (CCK-8) according to its protocol (Vazyme). Briefly, the corresponding cell lines infected with the control or sgRNAs were seeded onto 96-well plates at a density of 1000 cells per well. During a 7-day culture period, 10 μl of the CCK-8 solution was added to cell culture once a day and incubated for 1 h. The resulting color was assayed at 450 nm using a microplate absorbance reader (Bio-Rad). Each assay was carried out in triplicates.

Cell migration and invasion assay

Cell migration was assessed using a 24-well transwell unit with polycarbonate membrane (pore size, 8 μm) (Corning) according to the manufacturer's protocol. The membrane was coated with Matrigel basement membrane matrix (1 μg/μl) (BD Bioscience) for 24 h. Then Cells (0.5-2.5×104) were seeded into the upper chamber in a serum-free medium. The lower chamber was filled with a medium containing 10% FBS. After 24 h of incubation, the cells in the upper chamber were removed, and the cells were fixed in 4% paraformaldehyde, stained with crystal violet for 20 min. After being washed with water three times, digital images were obtained from the membranes, and cell areas were selected using the Scan Scope CS system (Aperio Technologies). The migrating cells were quantified in five randomly selected fields in each membrane, and the average value was defined as a migration or invasion index on three independent membranes. For invasion, the membranes utilized were Matrigel-coated invasion chambers (BD Biosciences) that were pre-hydrated in a serum-free medium.

Immunohistochemistry

Tissue microarrays (TMAs) were made using above 79 paired tissues in Shanghai Outdo Biotech Company (Shanghai, China), including tumor and adjacent normal tissues. The immunohistochemistry (IHC) was performed by the streptavidin-peroxidase method (Zymed Laboratories Inc., San Francisco, CA, USA). The FBXW7 antibody was purchased from ABclonal(A5872, China) and diluted into 1:1000. The MLST8 was purchased from Abclonal (A13599, China) and diluted into 1:1000. IHC scores were determined by the estimated proportion of positive tumor cells in percentage. Assess the average degree of staining within a tumor, multiple regions were analyzed, and at least 100 tumor cells were assessed. The H-score system assessed the cytoplasmic or nucleus expression. The H-score formula is Histoscore $=\sum(I \times Pi)$, where I = intensity of staining and Pi = percentage of stained tumor cells, producing a cytoplasmic score ranging from 0 to 200. The scoring was independently assessed by two assessors (AWHC and JHMT) who were unaware of the clinical outcomes.

Statistical analysis

Data were expressed as means ± SD. All experiments were carried out with three or more replicates. Statistical analyses were performed by Student's t-test for most studies and performed by using GraphPad Prism v7.0 software. A $P < 0.05$ was considered statistically significant.

Results

MLST8 is a potential biomarker for ccRCC according to TCGA

We first exploited the TCGA database to analyze MLST8 mRNA expression and its association with ccRCC prognosis. As shown in Fig. 1a, MLST8 was significantly upregulated in ccRCC samples compared to normal tissues at the transcriptional level ($p < 0.0001$). We next evaluated this association with clinical-pathological characteristics. Although there was no difference between MLST8 expression and lymphatic metastasis, MLST8 was correlated to tumor stage M stage (Fig. 1b-e). Because the N1 stage samples from TCGA were small, it was insufficient to demonstrate a correlation between MLST8 and N metastasis. However, a strong correlation was identified between the MLST8 expression and the overall survival of ccRCC patients (Fig. 1f, $p = 0.0248$). Therefore, we assumed that the non-significance between MLST8 and distant metastasis was potentially due to the limited sample size, necessitating future validation.

MLST8 is upregulated in ccRCC specimens and predicts poor clinical outcomes in ccRCC patients

To confirm the correlation between MLST8 expression and ccRCC progression, we performed immunohistochemistry (IHC) to assess the MLST8 protein expression in 79 human ccRCC specimens. Substantially overexpressed MLST8 protein was found in ccRCC specimens compared to adjacent normal tissue (Supplementary Table S2, $p < 0.0001$), and results showed a significant increase in the expression levels of MLST8 as ccRCC progressed to an advanced stage (Fig. 2a, b). The association

between MLST8 expression and clinical pathological characteristics are shown in Supplementary Table S2. The over-expression of MLST8 was strikingly correlated to the T stage ($p = 0.009$), TMN stage ($p = 0.058$), and Furman grade ($p < 0.0001$). However, there were no association between MLST8 expression levels and a patient's age, gender, and size. We developed Kaplan-Meier curves on 75 patients with a log-rank test for OS to elucidate the relationship between MLST8 expression and patients' survival in ccRCC. Our results reveal that a high expression of MLST8 is associated with poor OS (Fig. 2c, $p = 0.0183$). These results suggest that MLST8 is a potential prognostic marker in ccRCC.

FBXW7 interacts with MLST8

A previous study was performed quantitative mass spectrometry using FBXW7 knockout (KO) HCT116 cells [23]. Enrichment of MLST8 protein in the nuclear fraction of the HCT116 FBXW7-KO cells could be a binding partner for FBXW7, and most likely, the alpha isoform that resides in the nucleus (Figure 3a). To verify that FBXW7 is a *bona fide* MLST8 interactor, we first examined whether FBXW7 can interact with MLST8 cells. FLAG-FBXW7 and Myc-MLST8 constructs were co-expressed in 293T cells. Cells were subsequently harvested for co-immunoprecipitation (Co-IP) with the anti-FLAG antibody. As shown in Figure (Figure 3b), Myc-MLST8 was immunoprecipitated by FLAG-FBXW7, suggesting an exogenous interaction between these two proteins. Besides, a reciprocal Co-IP assay was performed using lysates of 293T cells that were co-transfected with FLAG-MLST8 and Myc-FBXW7 constructs. The results indicated that FLAG-MLST8 was also able to immuneprecipitate Myc-FBXW7 (Figure 3c). Then experiments further show that FLAG-FBXW7 was capable of immunoprecipitated endogenous MLST8 in 786-O cells (Figure 3d). We explored whether endogenous MLST8 and FBXW7 have an immediate interaction with each other. Immunoprecipitation using the anti-MLST8 antibody was performed using cell lysates prepared from 786-O cells. As shown in Figure 3e, endogenous FBXW7 was immunoprecipitated by MLST8, suggesting an endogenous interaction between these two proteins. Similarly, endogenous MLST8 was immunoprecipitated by FBXW7 (Figure 3f). To investigate whether FBXW7 co-localizes with MLST8 *in vivo*, 786-O, and A498 cells were transfected with FLAG-MLST8 and Myc-FBXW7, immunostained and visualized by confocal microscopy. As shown in Figure 3g, FBXW7 and MLST8 were co-localized in the nucleus. Taken together, these results indicate that FBXW7 forms a complex with MLST8 in cells.

MLST8 is degraded and ubiquitinated by tumor suppressor FBXW7

We next sought to investigate the mechanism by which FBXW7 regulates the protein levels of MLST8. Myc-FBXW7α and Flag-MLST8 were co-transfected in 293T cells, followed by treatment with DMSO and MG132, respectively. Although Myc-FBXW7α promoted the degradation of MLST8, this effect was inhibited by the treatment with the proteasome inhibitor MG132 (Figure 4a). We used CRISPR-Cas9 to knockout endogenous copies of FBXW7 in 786-O and A498 cells with two FBXW7-specific sgRNAs, resulting in an increase in MLST8 protein levels (Figure 4b) but no effect on the mRNA expression (Figure 4c). Further results showed that the depletion of FBXW7 significantly extends the half-life of endogenous MLST8 protein and stabilizes the levels of the MLST8 protein (Figure 4d-4e). Furthermore, when 786-O

cells were transfected with three isoforms (α, β, and γ) of FBXW7, all resulted in a marked reduction in the protein levels of MLST8 in a dose-dependent manner (Figure 4f). Since FBXW7 is an ubiquitinating enzyme, we wondered whether FBXW7 can ubiquitinate and downregulate MLST8 protein levels. As shown in Figure 4g, ectopic expression of FBXW7-WT, but not the FBXW7-△F-box mutant (catalytic inactive), decreased the protein levels of co-expressed MLST8 in a dose-dependent manner, suggesting that it's the ubiquitination activity of FBXW7 to promote MLST8 destabilization. Conversely, the depletion of FBXW7 using CRISPR-Cas9 knock out decreased MLST8 ubiquitination levels (Figure 4h), indicating that FBXW7 is responsible for MLST8 ubiquitination. Additionally, MLST8 protein was robustly polyubiquitinated in a dose-dependent manner when FBXW7-WT was co-expressed. By contrast, minimal or no MLST8 polyubiquitination was observed in FBXW7-△F-box expressing cells (Figure 4i). In sum, these data demonstrate that the FBXW7 E3 ubiquitin ligase complex regulates MLST8 protein stability through the ubiquitin-dependent proteasomal degradation pathway in ccRCC cell lines.

Thr50-dependent is required for FBXW7-mediated degradation of MLST8

The FBXW7-binding consensus motif (T/S)P*XX*(S/T/D/E) has been identified in several FBXW7 substrates, including cyclin E, c-Myc, c- Jun [9, 10], and OASIS [23]. When we examined the amino acid sequence of MLST8, we discovered that MLST8 harbors one perfectly matched (50-TPDRS-54) FBXW7-binding motif (Figure 5a-b). FBXW7 often recognizes phosphorylated Ser/Thr residues in the CPD motif. Therefore, we speculated that the regulation of MLST8 by FBXW7 might be mediated by the phosphorylation of Thr50 in its CPD. To examine whether this region is required for the FBXW7–MLST8 interaction, we generated MLST8 mutants in which the acidic residues T50 and S54 residues were mutated to Alanine. 293T cells were co-transfected with FBXW7α and MLST8-WT or MLST8 mutant. Although FBXW7 coimmunoprecipitated MLST8-WT at a similar level, both MLST8 mutant completely lost its FBXW7-binding capability (Figure 5c). These data indicate that the 50-TPDRS-54 motif is necessary for the FBXW7–MLST8 interaction. Next, we sought to identify whether the 50-TPDRS-54 motif is required for the FBXW7-mediated degradation of MLST8. As shown in Figure 5d, while FBXW7 efficiently targets MLST8-WT for degradation, the MLST8-T50A/S54A mutant displayed resistance to FBXW7-mediated degradation, indicating that the 50-TPDRS-54 motif is crucial to FBXW7-mediated MLST8 degradation. Furthermore, the T50A/S54A mutation prolonged the half-life of MLST8 protein (Figure 5e-f). Next, in vivo ubiquitination assays suggest that FBXW7 robustly enhanced the polyubiquitination of MLST8-WT, but not the MLST8-T50A/S54A mutant (Figure 5g). Consistent with the protein degradation, the T50A/S54A mutation largely diminished FBXW7 induced MLST8 ubiquitination. Therefore, these data demonstrate that the 50-TPDRS-54 motif functions as an MLST8 degron and is essential for FBXW7 binding and degradation through the ubiquitin-proteasome pathway.

Activated CDK1 induces degradation of MLST8 and decreases the binding with FBXW7 and MLST8

FBXW7-mediated degradation requires the phosphorylation of the first Ser/Thr in the CPD motif of FBXW7 target proteins by a variety of kinases, including GSK3β [24], CDK1/2 [22], CDK4, or CDK5 [25]. To identify the kinase involved in the phosphorylation of T50 in MLST8, we first analyzed the surrounding

amino acid sequence and found that Thr50 in MLST8 perfectly matches the general CDK1/2 consensus motif (S/TP*X*K/R) (26). WT-MLST8 expressed in 293T cells treated with phosphatase and proteasome inhibitors was detected by an anti-p-T50-MLST8 antibody, but this was not detected when using the T50A-MLST8 mutant (Figure 6a). Thus, the Thr50 of exogenous MLST8 is phosphorylated *in vivo*. Furthermore, we detected endogenous MLST8 and its phosphorylation on Thr50 in 786-O cells transfected with MLST8 Control (Figure 6b), suggesting that endogenous MLST8 was phosphorylated at Thr50 in 786-O cells. The CPD motif in MLST8 (Thr50-Pro51-Asp52-Lys53-Ser54) corresponds to the consensus motif for CDKs, which is Ser/Thr-Pro-*X*-Lys/Arg (Figure 6C). To identify the kinase responsible for phosphorylation of MLST8 at residue Thr50, we performed an *in vitro* phosphorylation assay using purified GST-MLST8 protein and recombinant cyclin-CDK complexes. Phosphorylation of Thr50 in mLST8 by a variety of kinases, including CDK5, CDK4, and CDK2, was not detected, but phosphorylation on a control RB protein was at the same efficiency (Figure 6d-e). CDK1 efficiently phosphorylated MLST8 at Thr50, while CDK2 slightly resulted in phosphorylation (Figure 6d). We also examined whether recombinant GSK3β phosphorylates GST-MLST8 *in vitro* (Figure 6f). We determined that GSK3β did not phosphorylate Thr50 in MLST8 *in vitro* and is not the kinase responsible for the CPD motif of MLST8. Furthermore, we investigated whether phosphorylation of Thr50 in MLST8 was required for its recognition by FBXW7 using a GST pull-down assay. Purified GST-WT-MLST8 or GST-T50A-MLST8 was phosphorylated by CDK1 and incubated with cell lysates expressing FLAG-FBXW7. MLST8 in the presence of CDK1 migrated more slowly than the unphosphorylated form of MLST8, even when Thr50 was mutated to alanine (T50A). we also found that FBXW7 bound to GST-WT-MLST8 was detected by an anti-p-T50-MLST8 antibody after treatment with CDK1, but did not bind to GST-MLST8 without CDK1(Figure 6g). Therefore, these results suggest that CDK1 phosphorylation of residue Thr50 in MLST8 is responsible for its recognition by FBXW7.

MLST8 is an important mediator of FBXW7 inactivation-induced cell proliferation, migration and invasion in vitro

Accumulating shreds of evidence showed that MLST8 expression was upregulated in various types of human cancers. This evidence drove us to explore whether MLST8 is involved in FBXW7 depletion-induced increase in cell proliferation, migration, and invasion. As determined by the CCK-8 assay, the growth rate of MLST8-depleted 786-O and A498 cells was slower than the control cells. In contrast, the depletion of FBXW7 could significantly enhance cell proliferation, and the phenotypes could be rescued by MLST8 co-depletion (Figure 7a-b). We observed similar effects as the cell proliferation assay, in which the increase of migration and invasion in 786-O and A498 cells by FBXW7 depletion was partly diminished by MLST8 inactivation (Figure 7C-D). Thus, these results suggest that MLST8 is an essential mediator of FBXW7 inactivation-induced cell proliferation, migration, and invasion.

MLST8 and FBXW7 Protein levels negatively correlate in human renal cancer specimens

Given the critical role of FBXW7 and MLST8 in ccRCC, we analyzed the expression of FBXW7 and MLST8 by IHC on a tissue microarray (TMA) in 79 pairs of renal cancer samples with clinical follow-up

information and observed that both are mainly expressed in the nucleus which is consistent with the result of immunofluorescence. Statistical analysis revealed that MLST8 was remarkably overexpressed in renal cancer tissues compared to normal tissue. In contrast, FBXW7 was expressed at a lower level in tumor tissues (Figure 8a**)**. The clinical and pathologic characteristics of the patients are shown in Supplementary Table. S2. In the 79 paired ccRCC cases, MLST8 protein was greatly overexpressed in 60.0% of tumor tissues, and FBXW7 was found to be under-expressed in 68.4% of tumor tissues (Figure 8b**)**. Moreover, statistical analysis indicated that MLST8 was negatively correlated with FBXW7 expression in this cohort of patient samples (r=-0.3124, p=0.0051) (Figure 8c**)**. This result suggested that FBXW7-mediated MLST8 decrease may also restrain renal cancer progression. Further, the univariate and multivariate analyses were used to determine the independent prognostic factors for ccRCC patients (Supplementary Table S3). In univariate analysis, the MLST8 expression level instead of FBXW7, was found to be significantly associated with the OS ($p = 0.006$). TNM stage ($p < 0.0001$) and Fuhrman grade ($p = 0.001$) were also correlated significantly with OS, nevertheless other factors such as tumor size ($p = 0.058$) and age ($p = 0.871$) were also uncorrelated significantly with OS. Moreover, multivariate analysis showed that the TNM stage ($p = 0.000$), tumor size ($p = 0.050$) were proven to be independent predictors of OS for ccRCC patients. Simultaneously, other variables, including age and Fuhrman grade, did not contribute to overall survival independently ($P > 0.05$).

Discussion

Over recent decades, aberrant activation of multiple signaling cascades, including the Hippo pathway, and the PI3K/Akt/mTOR pathway, are involved in the development and progression of ccRCC [1, 26]. The mTORC2 complex consists of mTOR, Rictor, Sin1 and MLST8[27], However, the role of MLST8, as a core member of the mTOR pathway, is unsettled in cases of ccRCC. In recent years, there have been multiple reports suggesting a role of MLST8 in malignancies, including colon and prostate cancer. Studies have shown that the overexpression of MLST8 suppresses tumor growth and invasion [4, 26]. Another study showed that MLST8 contributes to promoting cell proliferation and metastasis via the AKT pathway in HCC [14]. We observed that MLST8 upregulation was associated with the upregulation of other components of mTOR complexes, such as mTOR itself and RICTOR/RAPTOR. Therefore, MLST8 upregulation can be attributed to enhanced protein stabilization, which is in turn caused by the upregulation of binding partners that are modulated by other mechanisms, such as micro- RNA silencing[28]

Our study firstly detected MLST8 expression and analyzed its correlation with clinical factors in ccRCC patients. Our study identified that the overexpression of MLST8 was a frequent event in ccRCC specimens, which is in line with TCGA. We also have confirmed that increased MLST8 expression is predictive of an unfavorable prognosis for human renal cancer. Also, cellular functions and molecular mechanisms of MLST8 remain unknown in ccRCC. Ubiquitin-proteasome-dependent protein degradation usually requires the direct interaction between the substrate and an E3 ubiquitin ligase [29]. Fbw7 contains several conserved protein interaction domains. A stretch of eight WD40 repeats makes multiple contacts with the CPDs in the Fbw7 substrate [29]. Rapamycin binds to FK506 binding protein-12

(FKBP12), to form the FKBP12-rapamycin complex that only partially inhibits the mTOR kinase activity [30]. Recent study implies that concurrent targeting of mTORC1/2 by OSI-027 potently inhibits the proliferation and the migration of keloid keratinocytes[31]. Recent studies have implied that the concurrent targeting of mTORC1/2 by OSI-027 potently inhibits the proliferation and the migration of keloid keratinocytes[31]. Due to these limitations, direct mTOR kinase inhibitors have recently been developed and termed “second-generation mTOR inhibitors”[32]. In this study, we demonstrate for the first time that the WD40 domain of Fbw7 indeed binds to the CPD of MLST8. We note that the depletion of FBXW7 shows impaired binding to MLST8 proteins, resulting in impaired proteasomal degradation and the accumulation of MLST8 in renal cancer cell lines and cancer specimens, which partly contributes to FBXW7 inactivation-induced renal cancer cell migration and invasion. Interestingly, the exact mechanism by which CDK1, excluding the possibility of other protein kinases, phosphorylates MLST8 have also been determined.

As a shared subunit between mTORC1 and mTORC2, MLST8 may play a divergent role in the activation both mTORC1 and mTORC2. Genetic studies showed that the ablation of MLST8 in mice only influences mTORC2 function [6]. MLST8 protein inhibitors are emerging as promising anti-cancer therapies. The gene encoding the E3 ubiquitin ligase FBXW7 is the most frequently mutated gene in twenty CCA patients [6]. FBXW7 W406R and T416A are similar in activity to wild type FBXW7, while the mutants D510E and D527G degrade all targets with the exception of NOTCH1[33]. Hotspot mutations in FBXW7 have been reported for R505, R465 and R479, and represent 25.41%, 9.29% and 13.40%, respectively, of all FBXW7 mutations in cancer [34]. Mutations in FBXW7 that prevent BRAF degradation were associated with resistance to BET inhibitors [35]. FBXW7 mutant expression confers BET inhibitor resistance. These findings together with ours supported MLST8 act as an oncogene in renal cancer, and its protein and mRNA level were dysregulated in renal cancer. Development of therapeutic approaches for targeting aberrant MLST8 activation could be a viable treatment in renal cancer.

Conclusion

In conclusion, our results show that the upregulation of MLST8 exerts a decisive role in ccRCC progression. MLST8 is an independent predictive indicator for OS and provides novel insights into the aberrant regulation of MLST8 in renal cancer, suggesting that MLST8 is an important mediator of FBXW7 inactivation-induced cell proliferation, migration and invasion. This understanding will contribute to the elucidation of new strategies in developing substrate-specific FBXW7 inhibitors for therapeutic use.

Abbreviations

FBXW7: F-Box and WD Repeat Domain Containing 7 **MLST8**: MTOR Associated Protein **ccRCC**: clear cell renal cell carcinoma **UB**: ubiquitination enzymes **Co-IP**: co-immunoprecipitation **IHC**: Immunohistochemical **WB**: Western Blotting.

Declarations

Ethics approval and consent to participate

The institutional review board of Shanghai general hospital had approved the study by using formalin-fixed tissue. The Institutional Animal Care and Use Committee (IACUC) was from the Ethics Committee of General Hospital of Shanghai Jiao Tong University.

Funding

This study was completely supported by the National Natural Science Foundation of China (81570607).

Availability of data and materials

All data used and analyzed in this study are available from the corresponding author on request.

Authors' contributions

X. Wang, Q. Shi and M. Tan conceived and designed the study. E. Zhang, X. Dong and J. Shao performed experiments. E. Zhang wrote the paper. E. Zhang, X. Mu, S. Chen, P. Zhang and Y. Wang reviewed and edited the manuscript. All authors read and approved the manuscript.

Consent for publication

All authors agree for publication

Competing interests

The authors declare no potential conflicts of interest.

References

1. Saxton RA, Sabatini DM. mTOR Signaling in Growth, Metabolism, and Disease. Cell. 2017;168(6):960-76.
2. Janku F, Yap TA, Meric-Bernstam F. Targeting the PI3K pathway in cancer: are we making headway Nat Rev Clin Oncol. 2018;15(5):273-91.
3. Yu XN, Chen H, Liu TT, Wu J, Zhu JM, Shen XZ. Targeting the mTOR regulatory network in hepatocellular carcinoma: Are we making headway? Biochim Biophys Acta Rev Cancer. 2019;1871(2):379-91.
4. Kakumoto K, Ikeda J, Okada M, Morii E, Oneyama C. mLST8 Promotes mTOR-Mediated Tumor Progression. PLoS One. 2015;10(4):e0119015.
5. Yu XN, Zhang GC, Sun JL, Zhu HR, Shi X, Song GQ, et al. Enhanced mLST8 Expression Correlates with Tumor Progression in Hepatocellular Carcinoma. Ann Surg Oncol. 2020;27(5):1546-57.
6. Guertin DA, Stevens DM, Thoreen CC, Burds AA, Kalaany NY, Moffat J, et al. Ablation in mice of the mTORC components raptor, rictor, or mLST8 reveals that mTORC2 is required for signaling to Akt-

FOXO and PKCalpha, but not S6K1. Dev Cell. 2006;11(6):859-71.

7. Strohmaier H, Spruck CH, Kaiser P, Won KA, Sangfelt O, Reed SI. Human F-box protein hCdc4 targets cyclin E for proteolysis and is mutated in a breast cancer cell line. Nature. 2001;413(6853):316-22.
8. Zhang W, Koepp DM. Fbw7 isoform interaction contributes to cyclin E proteolysis. Mol Cancer Res. 2006;4(12):935-43.
9. Yada M, Hatakeyama S, Kamura T, Nishiyama M, Tsunematsu R, Imaki H, et al. Phosphorylation-dependent degradation of c-Myc is mediated by the F-box protein Fbw7. Embo j. 2004;23(10):2116-25.
10. Nateri AS, Riera-Sans L, Da Costa C, Behrens A. The ubiquitin ligase SCFFbw7 antagonizes apoptotic JNK signaling. Science. 2004;303(5662):1374-8.
11. Gupta-Rossi N, Le Bail O, Gonen H, Brou C, Logeat F, Six E, et al. Functional interaction between SEL-10, an F-box protein, and the nuclear form of activated Notch1 receptor. J Biol Chem. 2001;276(37):34371-8.
12. Sundqvist A, Bengoechea-Alonso MT, Ye X, Lukiyanchuk V, Jin J, Harper JW, et al. Control of lipid metabolism by phosphorylation-dependent degradation of the SREBP family of transcription factors by SCF(Fbw7). Cell Metab. 2005;1(6):379-91.
13. Akhoondi S, Sun D, von der Lehr N, Apostolidou S, Klotz K, Maljukova A, et al. FBXW7/hCDC4 is a general tumor suppressor in human cancer. Cancer Res. 2007;67(19):9006-12.
14. Akhoondi S, Lindstrom L, Widschwendter M, Corcoran M, Bergh J, Spruck C, et al. Inactivation of FBXW7/hCDC4-beta expression by promoter hypermethylation is associated with favorable prognosis in primary breast cancer. Breast Cancer Res. 2010;12(6):R105.
15. Ji S, Qin Y, Liang C, Huang R, Shi S, Liu J, et al. FBW7 (F-box and WD Repeat Domain-Containing 7) Negatively Regulates Glucose Metabolism by Targeting the c-Myc/TXNIP (Thioredoxin-Binding Protein) Axis in Pancreatic Cancer. Clin Cancer Res. 2016;22(15):3950-60.
16. Liang C, Qin Y, Zhang B, Ji S, Shi S, Xu W, et al. Oncogenic KRAS Targets MUC16/CA125 in Pancreatic Ductal Adenocarcinoma. Mol Cancer Res. 2017;15(2):201-12.
17. Arabi A, Ullah K, Branca RM, Johansson J, Bandarra D, Haneklaus M, et al. Proteomic screen reveals Fbw7 as a modulator of the NF-kappaB pathway. Nat Commun. 2012;3:976.
18. Kitagawa M, Okabe T, Ogino H, Matsumoto H, Suzuki-Takahashi I, Kokubo T, et al. Butyrolactone I, a selective inhibitor of cdk2 and cdc2 kinase. Oncogene. 1993;8(9):2425-32.
19. Kitagawa M, Higashi H, Takahashi IS, Okabe T, Ogino H, Taya Y, et al. A cyclin-dependent kinase inhibitor, butyrolactone I, inhibits phosphorylation of RB protein and cell cycle progression. Oncogene. 1994;9(9):2549-57.
20. Kitagawa K, Shibata K, Matsumoto A, Matsumoto M, Ohhata T, Nakayama KI, et al. Fbw7 targets GATA3 through cyclin-dependent kinase 2-dependent proteolysis and contributes to regulation of T-cell development. Mol Cell Biol. 2014;34(14):2732-44.

21. Kitagawa M, Higashi H, Jung HK, Suzuki-Takahashi I, Ikeda M, Tamai K, et al. The consensus motif for phosphorylation by cyclin D1-Cdk4 is different from that for phosphorylation by cyclin A/E-Cdk2. EMBO J. 1996;15(24):7060-9.
22. Nakajima T, Kitagawa K, Ohhata T, Sakai S, Uchida C, Shibata K, et al. Regulation of GATA-binding protein 2 levels via ubiquitin-dependent degradation by Fbw7: involvement of cyclin B-cyclin-dependent kinase 1-mediated phosphorylation of THR176 in GATA-binding protein 2. J Biol Chem. 2015;290(16):10368-81.
23. Yumimoto K, Matsumoto M, Onoyama I, Imaizumi K, Nakayama KI. F-box and WD repeat domain-containing-7 (Fbxw7) protein targets endoplasmic reticulum-anchored osteogenic and chondrogenic transcriptional factors for degradation. J Biol Chem. 2013;288(40):28488-502.
24. Koo J, Wu X, Mao Z, Khuri FR, Sun SY. Rictor Undergoes Glycogen Synthase Kinase 3 (GSK3)-dependent, FBXW7-mediated Ubiquitination and Proteasomal Degradation. J Biol Chem. 2015;290(22):14120-9.
25. Maskey D, Marlin MC, Kim S, Kim S, Ong EC, Li G, et al. Cell cycle-dependent ubiquitylation and destruction of NDE1 by CDK5-FBW7 regulates ciliary length. EMBO J. 2015;34(19):2424-40.
26. Shi X, Zhu HR, Liu TT, Shen XZ, Zhu JM. The Hippo pathway in hepatocellular carcinoma: Non-coding RNAs in action. Cancer Lett. 2017;400:175-82.
27. Sarbassov DD, Ali SM, Kim DH, Guertin DA, Latek RR, Erdjument-Bromage H, et al. Rictor, a novel binding partner of mTOR, defines a rapamycin-insensitive and raptor-independent pathway that regulates the cytoskeleton. Curr Biol. 2004;14(14):1296-302.
28. Oneyama C, Ikeda J, Okuzaki D, Suzuki K, Kanou T, Shintani Y, et al. MicroRNA-mediated downregulation of mTOR/FGFR3 controls tumor growth induced by Src-related oncogenic pathways. Oncogene. 2011;30(32):3489-501.
29. Welcker M, Clurman BE. FBW7 ubiquitin ligase: a tumour suppressor at the crossroads of cell division, growth and differentiation. Nat Rev Cancer. 2008;8(2):83-93.
30. Yu K, Toral-Barza L. Biochemical and pharmacological inhibition of mTOR by rapamycin and an ATP-competitive mTOR inhibitor. Methods Mol Biol. 2012;821:15-28.
31. Chen J, Liu K, Liu Y, Wang X, Zhang Z. Targeting mTORC1/2 with OSI-027 inhibits proliferation and migration of keloid keratinocytes. Exp Dermatol. 2019;28(3):270-5.
32. Zhou HY, Huang SL. Current development of the second generation of mTOR inhibitors as anticancer agents. Chin J Cancer. 2012;31(1):8-18.
33. Pancewicz J, Taylor JM, Datta A, Baydoun HH, Waldmann TA, Hermine O, et al. Notch signaling contributes to proliferation and tumor formation of human T-cell leukemia virus type 1-associated adult T-cell leukemia. Proc Natl Acad Sci U S A. 2010;107(38):16619-24.
34. Yeh CH, Bellon M, Nicot C. FBXW7: a critical tumor suppressor of human cancers. Mol Cancer. 2018;17(1):115.
35. Yeh CH, Bellon M, Wang F, Zhang H, Fu L, Nicot C. Loss of FBXW7-mediated degradation of BRAF elicits resistance to BET inhibitors in adult T cell leukemia cells. Mol Cancer. 2020;19(1):139.

Figures

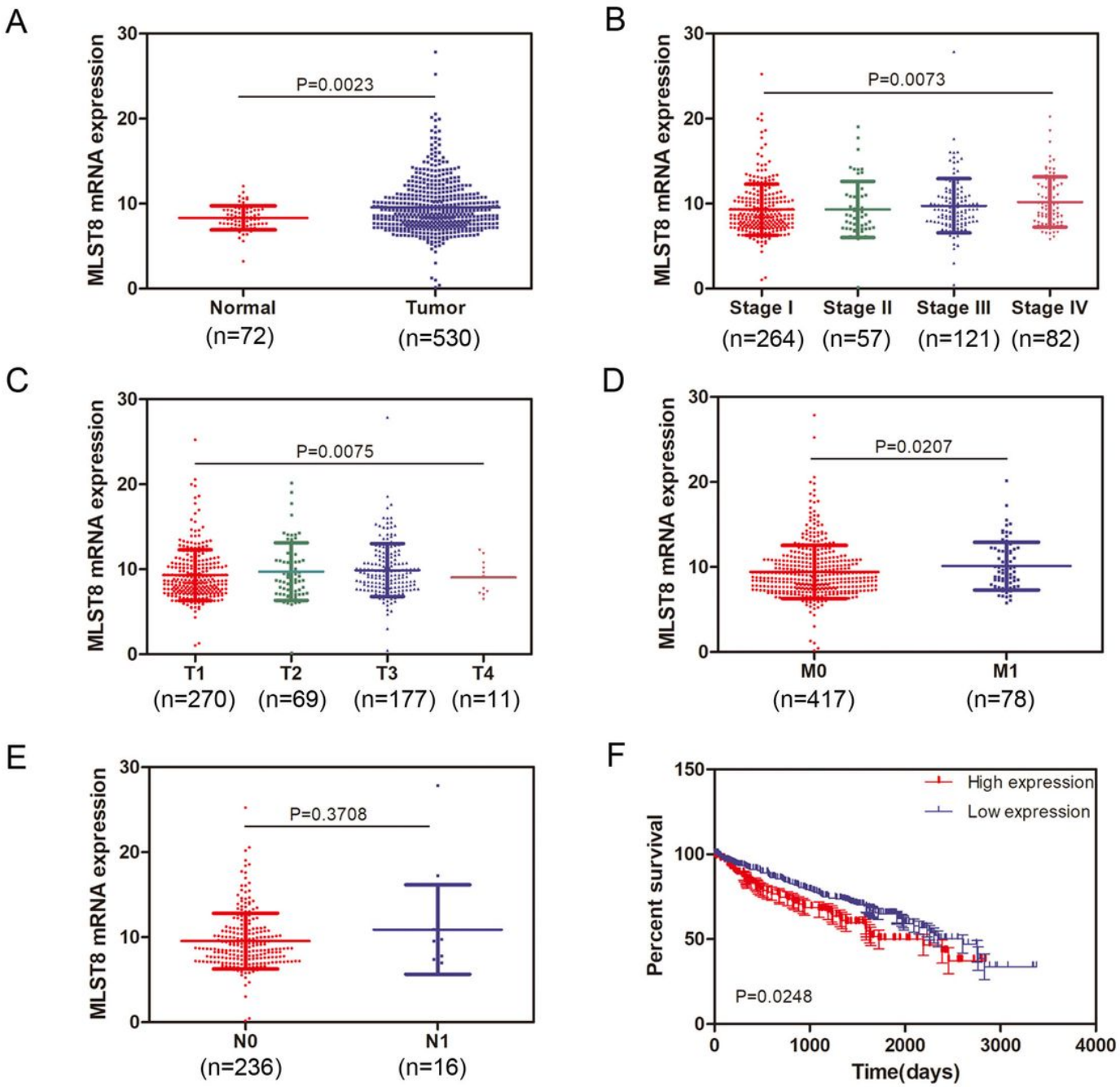

Figure 1

MLST8 is a potential biomarker for ccRCC according to TCGA. a Expression level of MLST8 in ccRCC was elevated in tumor tissues compared to normal tissue. b Expression of MLST8 was elevated gradually as ccRCC progressed to stage II and stage III. c Expression of MLST8 presented more upregulated in T2, T3 stage compared to that in T1. d Expression of MLST8 in ccRCC patients with M1 stage was remarkedly

increased compared that in M0 stage. e There was no significant difference of MLST8 expression between N1 stages and N0 stage in ccRCC patients. f OS curve of ccRCC patients based on MLST8 expression (p =0.0248). (The tumor stage was according to AJCC. T: Tumor, representing the extent of the primary tumor; N: lymph node, representing the presence or absence of regional lymph node metastasis; M: Metastasis, representing the presence or absence of distant metastases).

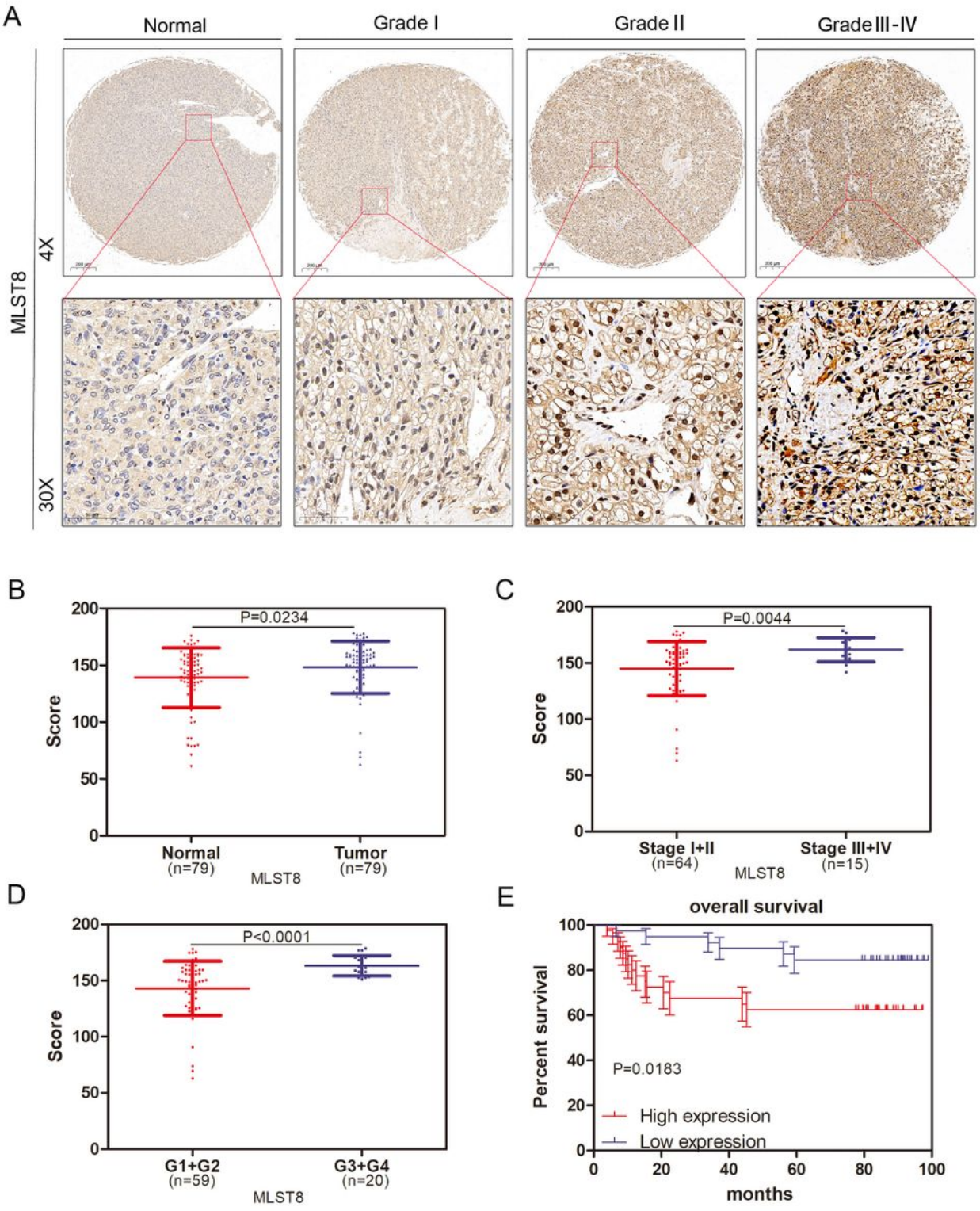

Figure 2

MLST8 is upregulated in ccRCC specimens and predicts poor clinical outcomes in ccRCC patients. a Expression of MLST8 increased as ccRCC progressed to more advanced stages. MLST8 protein expression was accessed by IHC analysis in 79 paired ccRCC specimens. b box plots of MLST8 protein expression based on their staining index in normal renal normal tissues and ccRCC specimens. c box plots of MLST8 protein expression based on different clinical stages. d box plots of MLST8 protein expression based on IS at different clinical stages. G1, G2, G3 and G4 represent well differentiated, moderately differentiated, and poorly differentiated tumors, respectively. e OS curve of ccRCC patients based on MLST8 expression according to Kaplan-Meier analysis. Patients with high levels of MLST8 were associated with poor survival(p=0.0183).

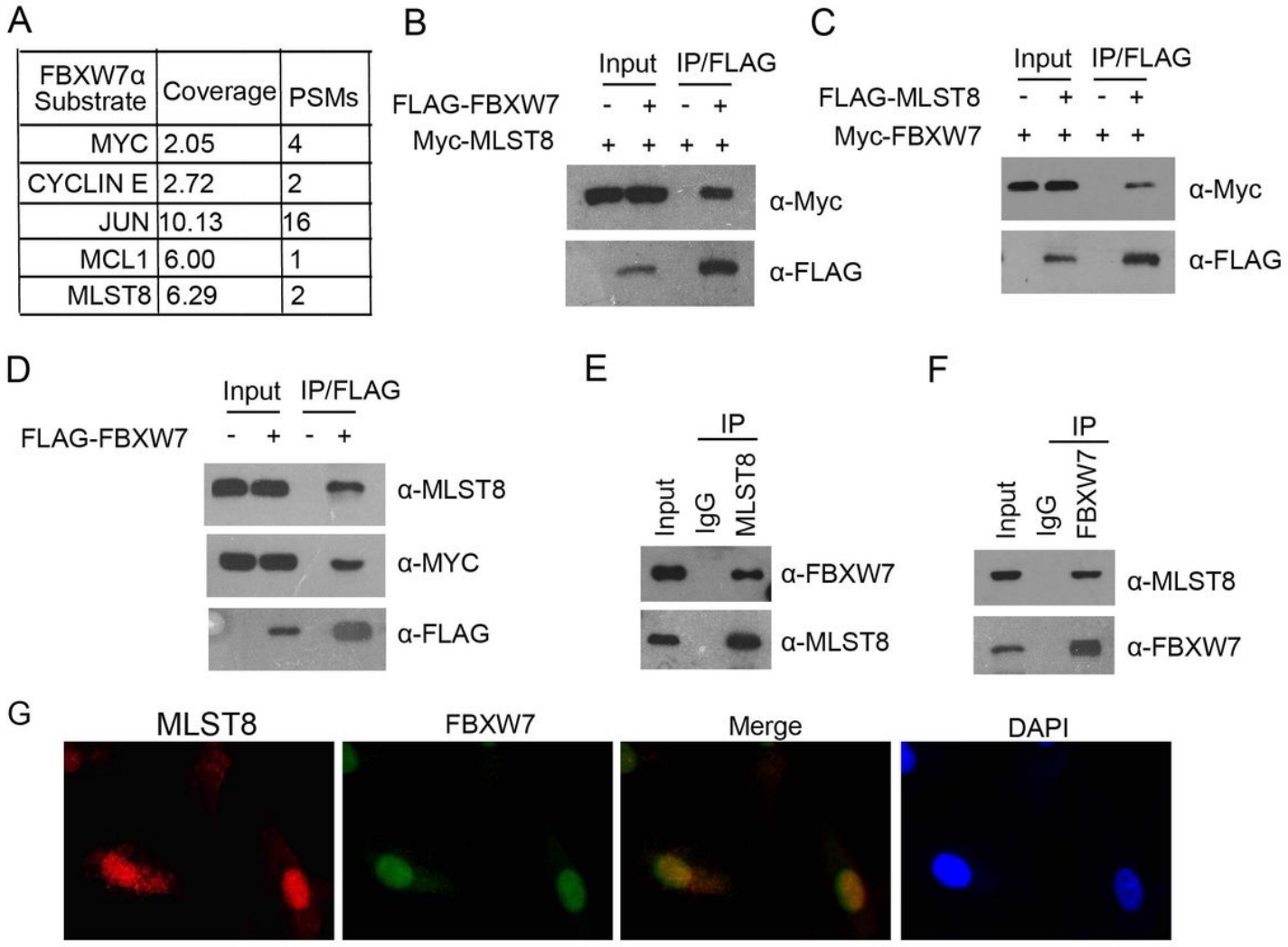

FBXW7α Substrate	Coverage	PSMs
MYC	2.05	4
CYCLIN E	2.72	2
JUN	10.13	16
MCL1	6.00	1
MLST8	6.29	2

Figure 3

FBXW7 directly interacts with MLST8. a quantitative mass spectrometry using FBXW7 knockout (KO) HCT116 cells. b, c 293T cells were co-transfected with Myc-MLST8 and FLAG-FBXW7 constructs. After 24 h, cell lysates were prepared for Co-IP with anti-FLAG antibody and Western blot¬ting. Similar coimmunoprecipitation assay was performed between Myc-FBXW7 and FLAG-MLST8. d Western blot

and co-IP samples of anti-FLAG antibody obtained from 293T cells infected with expressing FLAG-FBXW7 or control. The cells were treated with 20 μm MG132 for 8 h before harvesting. e, f After treated with 20 μm MG132 for 4 h, 786-O cell lysates were prepared for Co-IP with anti-MLST8 antibody and WB analyses with indicated antibodies. Similar Co-IP assay was performed with anti-FBXW7. g Confocal microscopy of 786-O cells stained with MLST8 and FBXW7 antibodies. DAPI represents nuclear staining. Red, green and blue channel images were captured by Olympus. Maximum projection images were shown and original magnification ×40.

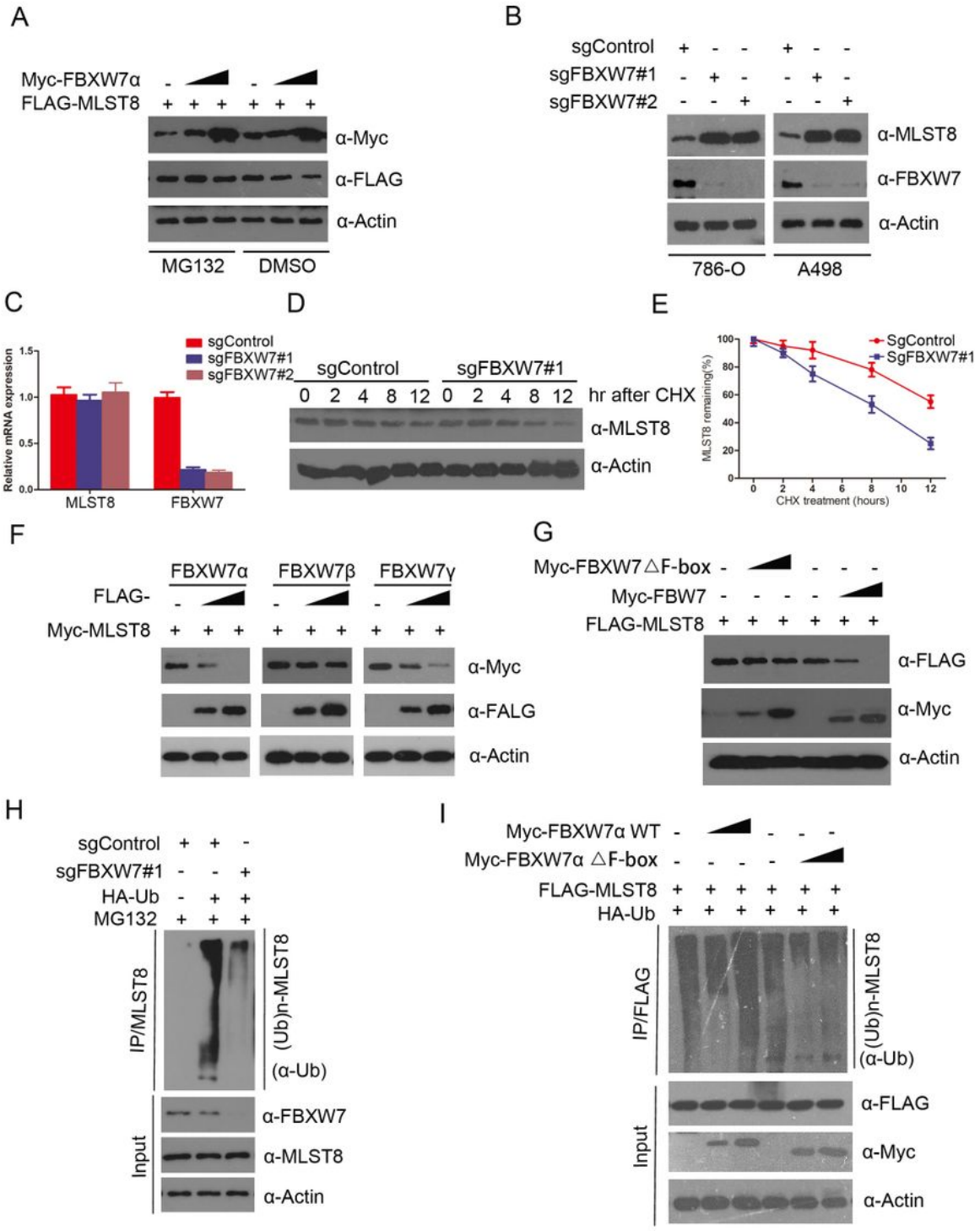

Figure 4

MLST8 is degraded and ubiquitination by tumor suppressor FBXW7. a Western blotting analysis of WCLs of 293T cells transfected with the indicated constructs. Cells were treated with or without 20μM MG132 for 8 h before harvest. b Western blot of indicated proteins in WCLs from 786-O and A498 cells with FBXW7 knockout through CRISPR/Cas9 methods. Parental 786-O and A498 cells were used as the control; Western blot of indicated proteins in WCLs from 786-O and A498 cells infected with lentivirus expressing FBXW7-specific sgRNA or negative control (NC). c RT-qPCR measurement of MLST8 mRNA expression in 786-O cells infected with lentivirus expressing FBXW7-specific sgRNA or NC; RT-qPCR measurement of MLST8 mRNA expression in parental and FBXW7-KO 786-O cells. Data are shown as means ± SD (n = 3). d, e Western blot of indicated proteins in WCLs of 786-O cells infected with lentivirus expressing FBXW7-specific sgRNA or NC for 48 h and then treated with 50 μg/ml cycloheximide (CHX) and harvested at different time points (d). At each time point, the intensity of MLST8 was normalized to the intensity of actin and then to the value at 0 h (e). Similar results were obtained from two independent experiments. f 786-O cells were transfected with the indicated plasmids for 24 h, followed by Western blotting analysis. g 786-O cells were transfected with the indicated plasmids for 24 h, followed by Western blotting analysis. h Western blot of indicated proteins in WCLs from 786-O with FBXW7 knockout through CRISPR/Cas9 methods, followed by treatment with 20 μM MG132 for 8 h. Immunoprecipitated MLST8 proteins were analyzed by WB for ubiquitination. i 786-O cells were transfected with the indicated plasmids for 16 h, followed by treatment with 20μM MG132 for 8 h. Immunoprecipitated FLAG-MLST8 proteins were analyzed by WB for ubiquitination.

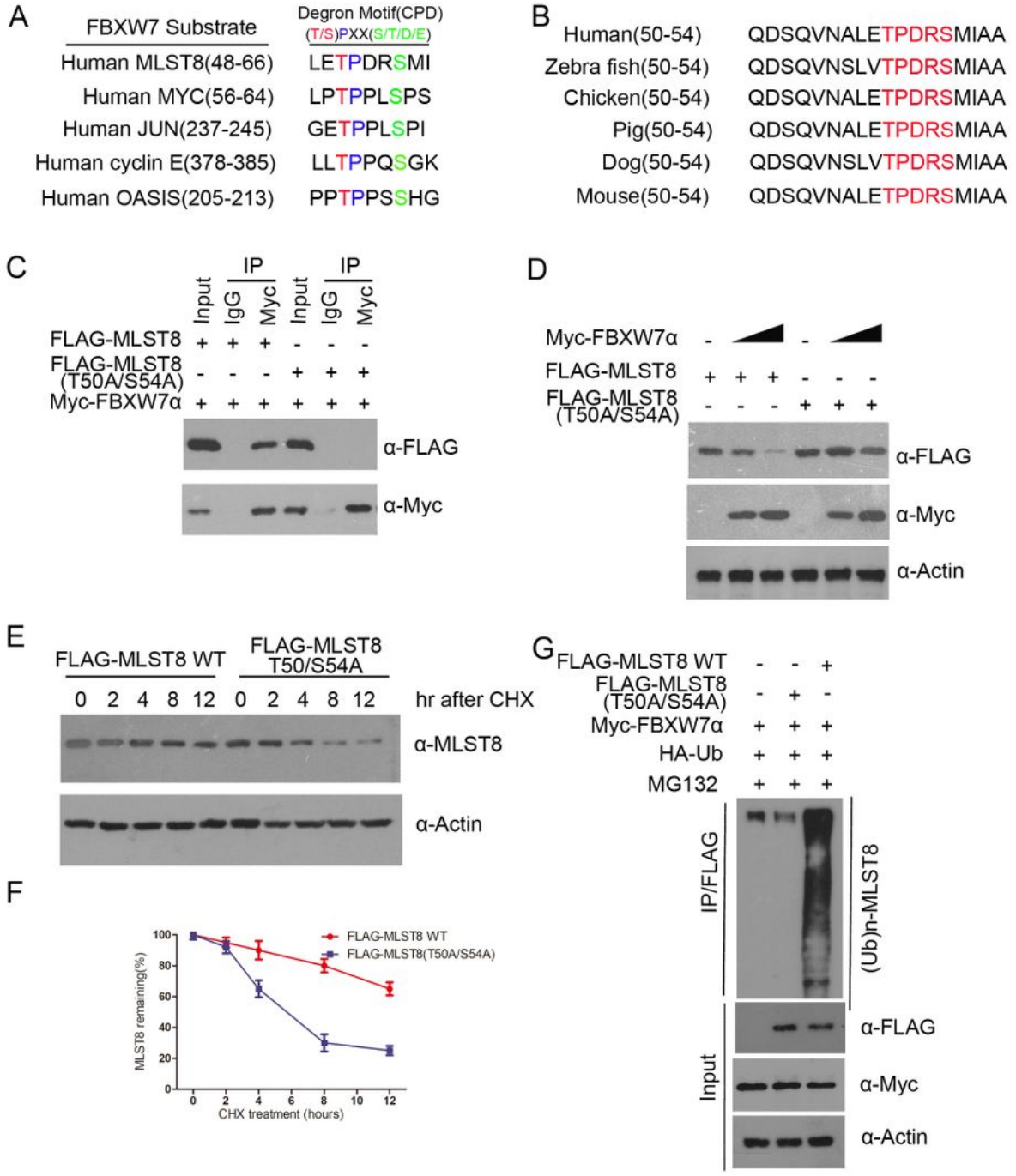

Figure 5

Thr50-dependent is required for FBXW7-mediated degradation of MLST8. a comparison of FBXW7 binding sites in MLST8 with the FBXW7-binding consensus motif defined in the known FBXW7 substrates. b schematic of conserved CPD motifs in MLST8 in different species. c Western blotting analysis of co-immunoprecipitation of ectopically expressed FLAG-MLST8 WT and FLAG-MLST8 T50A/S54A and Myc-FBW7α in 293T cells. d 786-O cells were transfected with the indicated plasmids for

24 h, followed by Western blotting analysis. e, f 786-O cells were transfected with the indicated plasmids. After 24 h, cells were treated with 50 μg/ml CHX. At different time points, cells were harvested for Western blotting analysis. g 786-O cells were transfected with the indicated plasmids for 16 h, followed by treatment with 20 μm MG132 for 8 h. Immunoprecipitated FLAG-MLST8 proteins were analyzed by WB for ubiquitination.

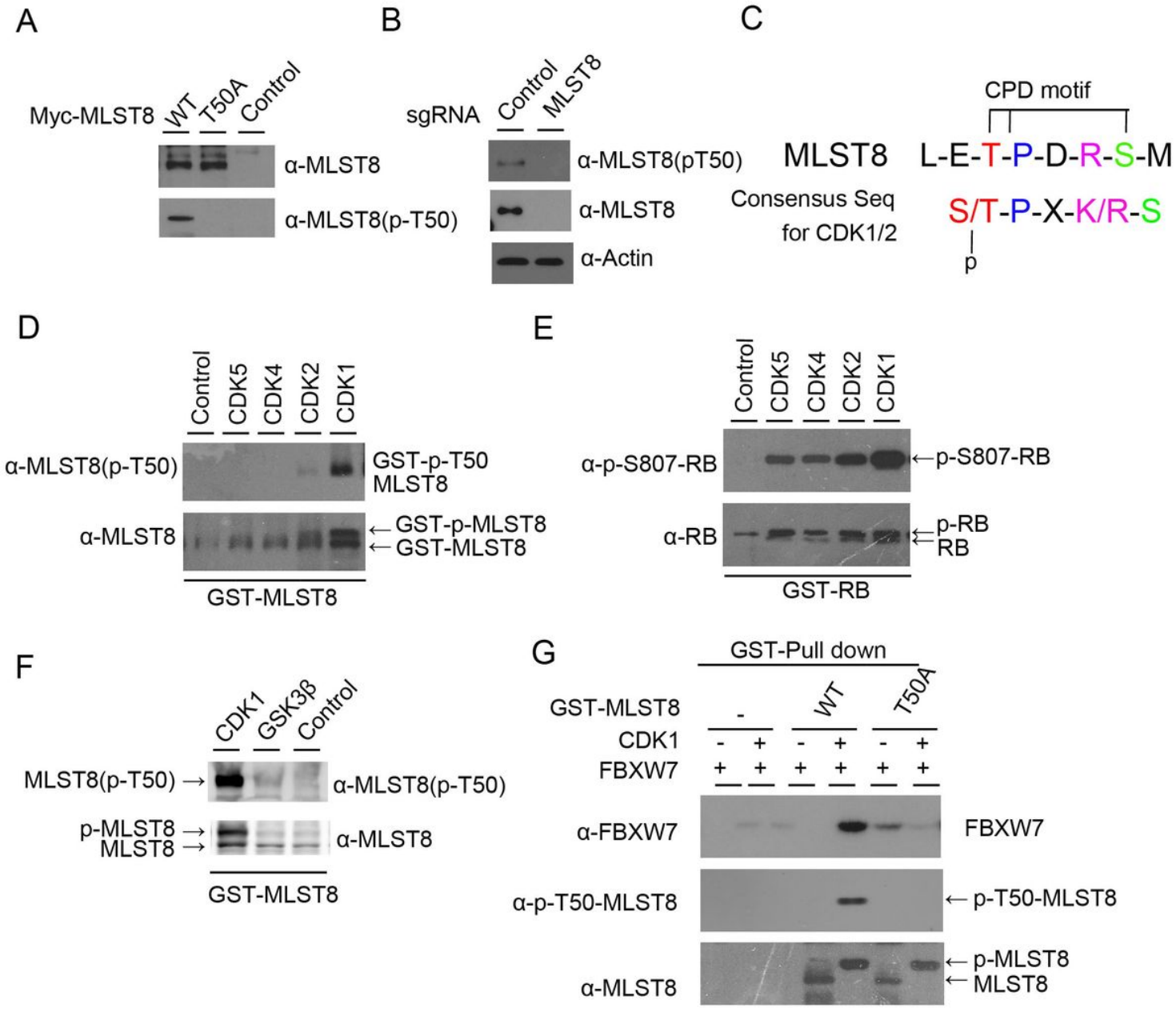

Figure 6

Activated CDK1 induces degradation of MLST8 and decreases the binding with FBXW7 and MLST8. a evaluation of antibodies against phospho-Thr50-MLST8 (p-T50-MLST8). WT-MLST8-myc, or T50A-MLST8-myc were transiently expressed in HEK293 cells. Cell lysates prepared with lysis buffer containing phosphatase inhibitors were subjected to immunoblotting with anti-MLST8 or anti-p-T50-MLST8. b Thr50 of endogenous MLST8 protein is phosphorylated in 786-O cells. Endogenous MLST8 protein was

depleted by MLST8-sgRNA, and lysates were subjected to immunoblotting with the indicated antibodies. c putative consensus motif for phosphorylation by CDK1 and CDK2 in the CPD motif containing Thr50 in MLST8. d, f Thr50 in MLST8 is efficiently phosphorylated by CDK1 in vitro. Recombinant GST-WT-MLST8 or GST-RB was incubated with the indicated recombinant kinases in reaction buffer with 1mM ATP for 30 min and then subjected to immunoblotting with the indicated antibodies. g Thr50-phosphorylated MLST8 binds FBXW7 in vitro. Purified GST-fused WT- or T50A-MLST8 or GST protein using glutathione beads was incubated with or without recombinant CDK1 in reaction buffer containing 1mM ATP for 30 min. The reaction mixtures were incubated with lysates from HEK293 cells expressing FLAG-FBXW7 and then precipitated using glutathione-Sepharose beads and subjected to IB with the indicated antibodies.

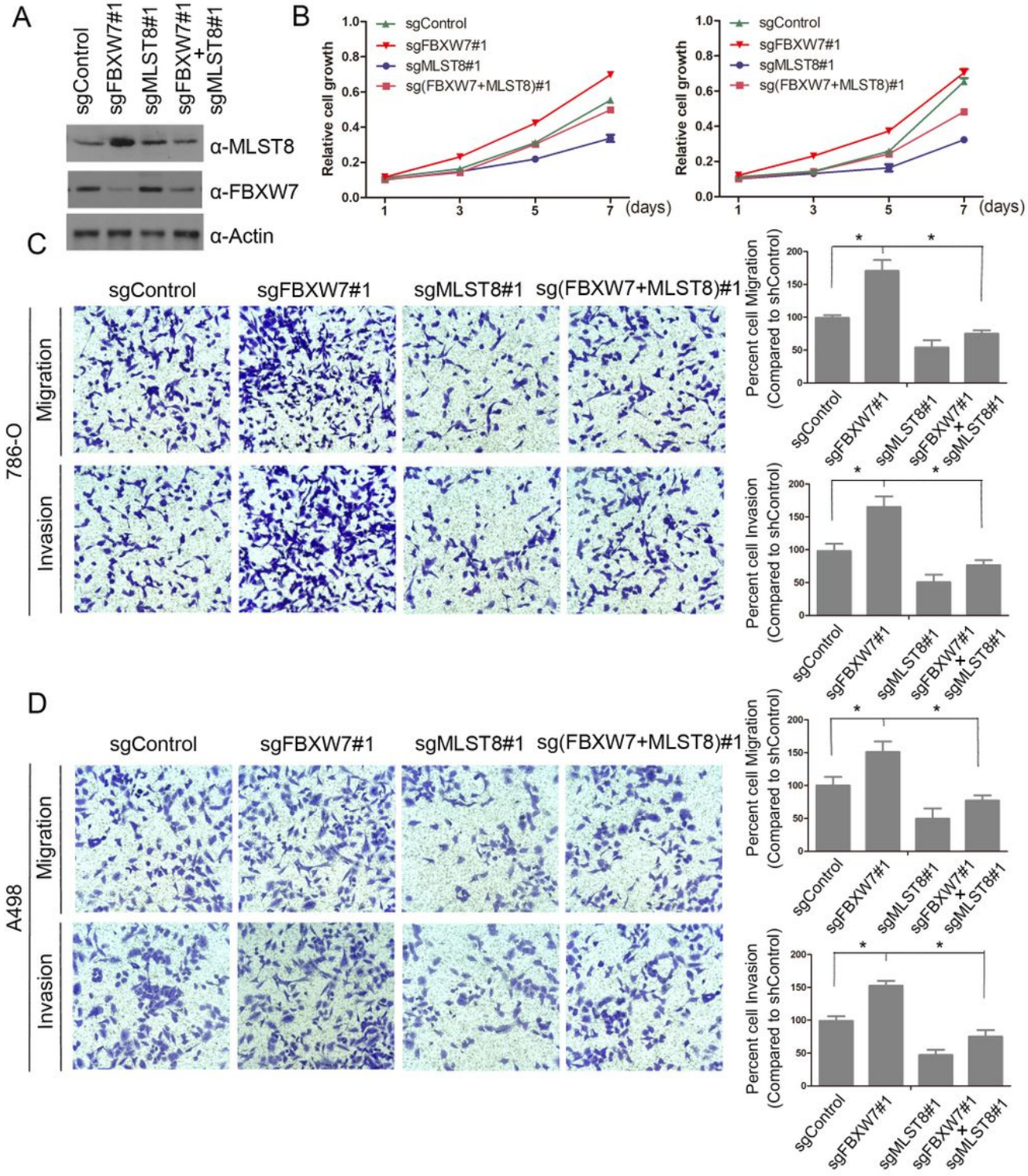

Figure 7

MLST8 is an important mediator of FBXW7 inactivation-induced cell proliferation, migration and invasion in vitro. a, b Western blot and CCK8 cell proliferation assay of parental or FBXW7 and(or) MLST8 knockout 786-O and A498 cells. Standard deviation (S.D.) of at least three independent experiments is shown to indicate statistical signifi¬cance. * represent P < 0.05. c-f Cell migration and invasion assays of parental or FBXW7 and(or) MLST8 knockout 786-O and A498 cells. Representative images of cell

migration and invasion assays were shown on the left panel, and the quantitative analysis is shown on the right panel. The mean values (S.D.) of three independent experiments are shown (*, P < 0.05).

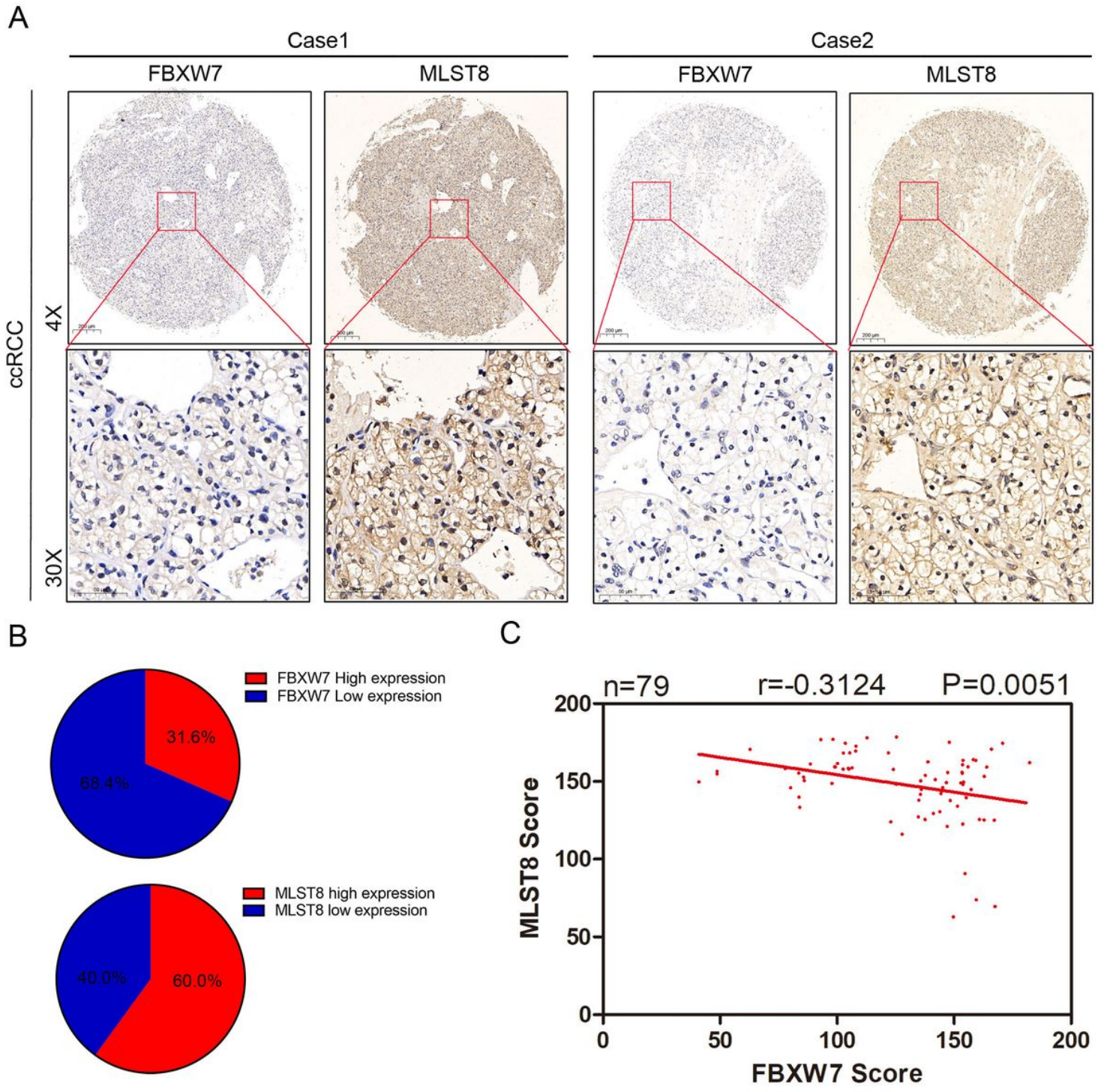

Figure 8

MLST8 and FBXW7 Protein levels negatively correlate in human renal cancer specimens. a Representative staining of IHC analysis of MLST8 and FBXW7 protein expression on tissue microarray (n=79 paired renal cancer tissue specimens). b FBXW7 and MLST8 staining patterns in 79 paired ccRCC

cases. c the negative correlation of FBXW7 and MLST8 protein expression was observed in human renal cancer specimens (Pearson's test, p <0.01).

Supplementary Files

This is a list of supplementary files associated with this preprint. Click to download.

- SupplementaryTableS1.docx
- SupplementaryTableS2.docx
- SupplementaryTableS3.docx